Arch Toxicol (2012) 86:779–790
DOI 10.1007/s00204-012-0801-y

REPRODUCTIVE TOXICOLOGY

Reversible aberration of neurogenesis targeting late-stage progenitor cells in the hippocampal dentate gyrus of rat offspring after maternal exposure to acrylamide

Bunichiro Ogawa · Liyun Wang · Takumi Ohishi · Eriko Taniai · Hirotoshi Akane · Kazuhiko Suzuki · Kunitoshi Mitsumori · Makoto Shibutani

Received: 3 August 2011 / Accepted: 4 January 2012 / Published online: 18 January 2012

Abstract We have recently shown that maternal exposure to acrylamide (AA) impaired neurogenesis in rat offspring measured by the increase in interneurons producing reelin, a molecule regulating migration and correct positioning of developing neurons, in the hippocampal dentate gyrus. To clarify the cellular target of AA on hippocampal neurogenesis and its reversibility after maternal exposure, pregnant Sprague–Dawley rats were given drinking water containing AA at 0, 4, 20, 100 ppm on day 10 of pregnancy through day 21 after delivery on weaning. Male offspring were examined immunohistochemically on postnatal day (PND) 21 and PND 77. For comparison, male pups of direct AA-injection control during lactation (50 mg/kg body weight, intraperitoneally, 3 times/week) were also examined. On PND 21, maternal AA-exposure decreased progenitor cell proliferation in the subgranular zone (SGZ) from 20 ppm accompanied with increased density of reelin-producing interneurons and NeuN-expressing mature neurons within the hilus at 100 ppm, similar to the direct AA-injection control. In the SGZ examined at 100 ppm, cellular populations immunoexpressing doublecortin or dihydropyrimidinase-like 3, suggesting postmitotic immature granule cells, were decreased. On PND 77, the SGZ cell proliferation and reelin-producing interneuron density recovered, while the hilar mature neurons sustained to increase from 20 ppm, similar to the direct AA-injection control. Thus, developmental exposure to AA reversibly affects hippocampal neurogenesis targeting the proliferation of type-3 progenitor cells resulting in a decrease in immature granule cells in rats. A sustained increase in hilar mature neurons could be the signature of the developmental effect of AA.

Keywords Acrylamide · Neuronal development · Hippocampal dentate gyrus · Impaired neurogenesis · Immunohistochemistry · Reversibility

Abbreviations

AA	Acrylamide
Actb	Beta actin
C_T	Threshold cycle
Dcx	Doublecortin
Dpysl3	Dihydropyrimidinase-like 3
GABA	Gamma-aminobutyric acid
GAD67	Glutamic acid decarboxylase 67
Gapdh	Glyceraldehyde-3-phosphate dehydrogenase
GD	Gestational day
NeuroD1	Neurogenic differentiation 1
NeuN	Neuron-specific nuclear protein
Pax6	Paired box 6
PCNA	Proliferating cell nuclear antigen
PND	Postnatal day
SGZ	Subgranular zone
Tbr2	T-box brain protein 2
TUNEL	Terminal deoxynucleotidyl transferase dUTP nick end labeling

Electronic supplementary material The online version of this article (doi:10.1007/s00204-012-0801-y) contains supplementary material, which is available to authorized users.

B. Ogawa · L. Wang · T. Ohishi · E. Taniai · H. Akane · K. Suzuki · K. Mitsumori · M. Shibutani (✉)
Laboratory of Veterinary Pathology,
Tokyo University of Agriculture and Technology,
3-5-8 Saiwai-cho, Fuchu-shi, Tokyo 183-8509, Japan
e-mail: mshibuta@cc.tuat.ac.jp

E. Taniai
Pathogenetic Veterinary Science,
United Graduate School of Veterinary Sciences,
Gifu University, 1-1 Yanagido, Gifu-shi, Gifu 501-1193, Japan

Introduction

Acrylamide (AA) is a water-soluble vinyl monomer that is used primarily to produce polymers (polyacrylamides) that have broad applications in the chemical industry for water management, ore processing, and dye synthesis, as well as its use in experimental laboratories conducting molecular biology studies and/or biochemistry (LoPachin 2004; Lee et al. 2005). AA has been shown to be a neurotoxicant, reproductive toxicant, and genotoxic carcinogen in animal species (Exon 2006; WHO/IPCS 2006). Exposure to AA in foodstuffs has become a worldwide concern recently because of its generation in a variety of fried and oven-baked foods during cooking through Maillard reactions of sugars with asparagine residues (Mottram et al. 2002).

In the nervous system, it is well known that AA targets axon terminals in both the central and peripheral nervous systems as represented by distal axonopathy (LoPachin 2004). However, developmental exposure to AA by maternal transfer, at dose levels inducing maternal neurotoxicity, has shown no such neurotoxicity in offspring but results in a reduced body size by us and others (Friedman et al. 1999; Takahashi et al. 2009). On the other hand, direct injection of AA into neonatal rats throughout the lactation period resulted in neurotoxicity similar to that observed in adult animals (Takahashi et al. 2009), suggesting that neonates and adult animals have comparable sensitivity with AA. The lack of neurotoxicity of AA in maternally exposed pups was considered to be due to limited lactational transfer and perhaps to impairment in nursing/lactation activity as a consequence of maternal neurotoxicity (Takahashi et al. 2009), which might also explain the loss of offspring body weight.

Within the brain, the dentate gyrus in the hippocampal formation is a unique structure that can continue neurogenesis during postnatal life (Zhang et al. 2009). The postnatal neurogenesis (so-called "adult neurogenesis") occurs in the neuroblast-producing subgranular zone (SGZ) from the type-1 progenitor cells and produces intermediate generations in the order of type-2a, type-2b, and type-3 cells in the SGZ. Then, type-3 cells undergo final mitosis to differentiate to immature granule cells, and then to mature granule cells (Hodge et al. 2008). In addition, γ-aminobutyric acid (GABA)ergic interneurons in the hilus of the dentate gyrus produce reelin in the embryonic period and throughout adult life to regulate the migration and maturation of newborn granule cells in the granule cell layer (Lussier et al. 2009). In our laboratory, increase in reelin-producing interneurons in the hilus has recently been shown in a rat model of neuronal mismigration induced by developmental hypothyroidism (Saegusa et al. 2010). Recently, increasing numbers of chemicals have revealed to affect proliferation and differentiation of progenitor cells by exposure to mice or rats during postnatal life (Choi et al. 2011; Hwang et al. 2011; Nam et al. 2011; Yan et al. 2011; Yoo et al. 2011). Because neurogenesis in the dentate gyrus is rather active during the developmental stage than the adult stage, developmental exposure to such chemicals may risk stronger impact on neurogenesis. Therefore, it may be reasonable to analyze neuronal stage-defining markers in combination with reelin-producing interneurons for elucidation of the influence of exogenously administered chemicals on neurogenesis as well as the target cell affected.

It is well established that the molecular mechanisms controlling neuronal migration during development have many similarities with those described for axon guidance (Nóbrega-Pereira and Marín 2009), suggesting that both migrating neuroblasts and immature axon terminals may be sensitive to AA. In our recent study, developmental exposure effect of AA on neurogenesis has been examined using samples verified as lacking any obvious axon terminal injury (Takahashi et al. 2009). The offspring of maternally exposed AA through drinking water (25, 50, 100 ppm) showed an AA dose-dependent increase in the density of reelin-immunoreactive GABAergic interneurons, suggesting an affection of neurogenesis and following neuronal migration (Ogawa et al. 2011). The lowest-observed adverse effect level of AA was determined to be 25 ppm by maternal exposure (3.72 mg/kg body weight/day). Although AA-exposed offspring had reduced body size, it has already been confirmed that there was no influence of systemic growth retardation during development using an intrauterine growth retardation model on the distribution of reelin-synthesizing interneurons in the hilus and the neurogenesis in the SGZ by us (Ohishi et al. 2010).

This study further investigates developmental exposure effect of AA on neuronal development in rat offspring. The reversibility of the aberration in neurogenesis was examined at the adult stage, as well as the target progenitor cell of AA in the SGZ employing a line of neuronal stage-defining markers. To measure the immunoreactive cell populations in the substructure of the dentate gyrus, a profile counting method was applied (Lussier et al. 2009).

Materials and methods

Chemicals and animals

Acrylamide was purchased from Sigma Chemical Co. (St. Louis, MO, USA; CAS #79-06-1) with a purity of more than 98%. Pregnant Sprague–Dawley rats were purchased from Japan SLC, Inc. (Hamamatsu, Japan) at gestational day (GD) 3 (the day when a vaginal plug was observed was designated as GD 0). They were housed individually in

polycarbonate cages with wood chip bedding, in an air-conditioned animal room on a 12 h light–dark cycle and conditioned at 23 ± 2°C with a relative humidity of 55 ± 15%. Animals were provided with pelleted basal diet (MF diet; Oriental Yeast Co., Ltd., Tokyo, Japan) and tap water ad libitum during the 7-day acclimatization period.

Experimental design

Two experiments were carried out. In Experiment 1, dams received AA. Twenty-four dams were randomly divided into four groups of 6 dams each and given AA at either 0, 4, 20, 100 ppm in the drinking water from GD 10 to day 21 after delivery. The highest dose was selected as that inducing progressive neurotoxicity to dams in our previous study (Takahashi et al. 2009). In Experiment 2, AA was administered directly to delivered neonates. Sixteen dams were divided into two groups of 8 dams, all maintained untreated until delivery. Neonates received vehicle saline (control) or AA at 50 mg/kg BW by intraperitoneal (ip) injections 3 times a week from postnatal day (PND) 4 to 21 (where PND 0 is the day of delivery). This AA dosing regimen has been shown to induce degeneration of the sciatic nerve in adult rats within 3 weeks (Saita et al. 1996). Each dam was housed with her litter individually, and body weights and food and water consumption were measured regularly. Litter size, sex, and body weight of pups were checked at PND 2, and litters were culled to preserve eight male pups per dam at PND 4. Female pups were included to maintain a total of eight pups/litter if dams had fewer than eight male pups. Culled female pups were killed by rapid decapitation. Daily observation was conducted for clinical signs, including gait abnormalities and mortality of dams and offspring, throughout the experimental period.

To assess AA-induced neurological abnormalities, all animals in the AA-treated and untreated groups were scored with respect to the appearance of gait abnormalities as described previously (Lee et al. 2005). The degree of abnormality was classified into the following 4 categories: Grade 1 as normal gait; Grade 2 as slightly abnormal gait with slight degrees of ataxia, hopping gait, and foot splay; Grade 3 as moderately abnormal gait with moderate degrees of ataxia, foot splay, and limb abduction; Grade 4 as severely affected gait including inability to support the BW as well as foot splay.

On day 21 after delivery, necropsy was performed on all dams and 3–4 male pups/litter after deep anesthesia with ether to remove brains for immunohistochemical analysis (dams and pups) and real-time RT-PCR analysis (pups). The livers of dams were also removed for weight measurement. The remaining male pups were allocated to 4 rats per cage without any special treatments or administrations, and necropsy was performed to remove their brains after ether anesthesia on PND 77.

For immunohistochemical analysis, the brains of 10–12 male pups/group (1–2 pups/litter, mostly 2 pups/litter) were fixed at both PND 21 and PND 77 in Bouin's solution at room temperature overnight in both Experiment 1 and Experiment 2. Then, coronal brain slices were routinely processed approximately at the position of −2.9 mm from the bregma at PND 21 and −3.3 mm at PND 77 for paraffin embedding. Serial sections at 5 μm were prepared from the position of −3.1 mm from the bregma at PND 21 and −3.6 mm at PND 77. Immunohistochemistry was additionally performed on similarly fixed brains of female pups culled on PND 4 (9–10 pups/group; 1–2 pups/litter, mostly 2 pups/litter) in Experiment 1. For real-time RT-PCR analysis, brains of 6–12 male pups/group (1–2 pups/litter) removed on PND 21 were fixed in methacarn solution for 6 h and then dehydrated at 4°C overnight as described previously (Lee et al. 2006) in both Experiment 1 and Experiment 2. Then, coronal brain slices were made by cutting laterally at the positions of +1 mm and −5 mm from the bregma to dissect bilateral whole hippocampal tissues from slices using tweezers after removal of the cerebral cortical tissues. Dissected tissue samples were preserved in 99.5% ethanol at −80°C until use for real-time RT-PCR analysis.

All procedures of this study were conducted in compliance with the "Guidelines for Proper Conduct of Animal Experiments" (Science Council of Japan, June 1, 2006) and according to the protocol approved by the Animal Care and Use Committee of the Tokyo University of Agriculture and Technology.

Immunohistochemistry and apoptosis assays

Immunohistochemistry was performed on the brains of offspring and dams for the detection of reelin, proliferating cell nuclear antigen (PCNA), neuron-specific nuclear protein (NeuN), and neuronal stage-defining markers, dihydropyrimidinase-like 3 (Dpysl3, also known as TUC-4), doublecortin (Dcx), neurogenic differentiation 1 (NeuroD1), t box brain protein 2 (Tbr2, also known as Eomes), and paired box 6 (Pax6). Following primary antibodies were used for immunohistochemical analysis: reelin (mouse monoclonal, clone G10, 1:1,000; Novus Biologicals, Inc., Littleton, CO, USA), PCNA (mouse monoclonal, clone PC10, 1:200, Dako, Glostrup, Denmark), NeuN (mouse monoclonal, clone A60, 1:1,000, Chemicon, Billerica, MA, USA), Dpysl3 (rabbit polyclonal, 1:1,000, Chemicon), Dcx (rabbit polyclonal antibody, 1:2,000, Abcam Inc., Cambridge, UK), NeuroD1 (mouse monoclonal, 1:300, Abcam Inc.), Tbr2 (rabbit polyclonal, 1:500, Abcam Inc.), and Pax6 (mouse monoclonal, clone AD2.38, 1:500, Abcam Inc.). We applied a

horseradish peroxidase avidin–biotin complex method for immunodetection of antigens utilizing a VECTASTAIN® Elite ABC Kit (Vector Laboratories Inc., Burlingame, CA, USA) with 3,3′-diaminobenzidine/H_2O_2 as the chromogen. Antigen retrieval was performed with PCNA antibody by autoclaving deparaffinized sections at 121°C for 10 min in 10 mM citrate buffer (pH 6.0). No antigen retrieval was applied for other antibodies. Immunostained sections were counterstained with hematoxylin for microscopic examination. The animal groups examined for immunohistochemistry on each antigen were listed in Table 1.

Apoptotic bodies were detected by Cresyl Violet-staining (Nuñez and McCarthy 2004) to evaluate apoptosis in the dentate SGZ of pups. Terminal deoxynucleotidyl transferase dUTP nick end labeling (TUNEL) was carried out to confirm apoptosis using the ApopTag® Peroxidase In situ Apoptosis Detection kit (Millipore, Temecula, CA, USA). Animal groups examined are listed in Table 1.

Analysis of immunolocalization and apoptotic cells

Immunoreactive cells and apoptotic cells were counted by blind trial for the treatment conditions.

On both PND 21 and PND 77, positive cells showing reelin- or NeuN-immunoreactivity distributed in the dentate hilus were bilaterally counted and normalized for the number per unit area of the hilus as described previously in both Experiment 1 and Experiment 2 (Fig. 1; Saegusa et al. 2010; Ohishi et al. 2010). In the dentate SGZ, apoptotic bodies stained with Cresyl Violet were bilaterally counted, as well as cells showing nuclear immunoreactivity for PCNA, Dpysl3, NeuroD1, Tbr2, and Pax6, and TUNEL-positive cells and the number was normalized with the length of the granule cell layer measured. Dcx-positive cells showing cytoplasmic immunoreactivity was also counted and normalized similarly.

Reelin-positive cells distributed in the molecular layer or in the dentate hilus were bilaterally counted and the

Table 1 List of animal groups examined for immunohistochemistry and apoptosis assays

	Experiment 1				Experiment 2	
	AA in the drinking water (ppm)				Intraperitoneal injections	
	0 (control)	4	20	100	Saline (control)	AA
PND 21, male offspring						
Reelin	T	T	T	T	T	T
NeuN	T	T	T	T	T	T
PCNA	T	T	T	T	T	T
Dpysl3	T	NE	NE	T	NE	NE
Dcx	T	NE	NE	T	NE	NE
NeuroD1	T	NE	NE	T	NE	NE
Tbr2	T	NE	NE	T	NE	NE
Pax6	T	NE	NE	T	NE	NE
Cresyl Violet-staining	T	T	T	T	T	T
TUNEL-assay	O	O	O	O	O	O
PND 77, male offspring						
Reelin	T	T	T	T	T	T
NeuN	T	T	T	T	T	T
PCNA	T	T	T	T	T	T
Dpysl3	O	NE	NE	O	NE	NE
Dcx	O	NE	NE	O	NE	NE
Cresyl Violet-staining	T	T	T	T	T	T
PND 4, female offspring						
Reelin	O	O	O	O	O	O
Dams						
Reelin	T	NE	NE	T	NA	NA
PCNA	T	NE	NE	T	NA	NA

T stained three different sections with approximately 250-μm interval in each brain, *O* stained one section in each brain, *NE* not examined, *NA* not applicable

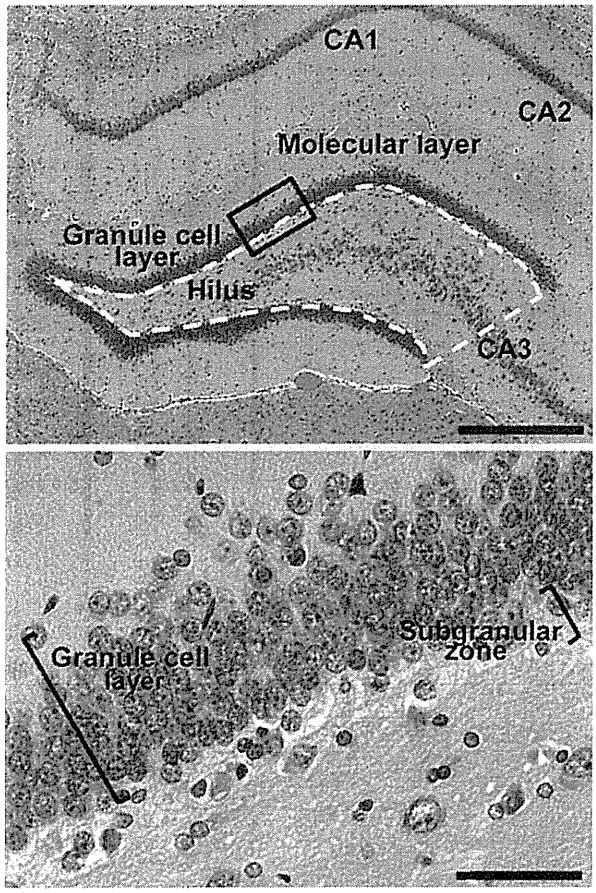

Fig. 1 Overview of the hippocampal formation of a male rat at PND 77 stained with hematoxylin and eosin. (*Upper panel*) Immunoreactive cells for reelin and NeuN were counted in the hilus of the dentate gyrus, as enclosed by the white dotted line. Magnification, ×40; *bar* 500 μm. (*Lower panel*) Higher magnification of the granule cell layer and SGZ as enclosed by the black line in the *upper panel*. Immunoreactive cells for PCNA, Pax6, Tbr2, NuroD1, Dcx, and Dpysl3, as well as apoptotic cells as detected by Cresyl Violet-staining and TUNEL-staining were measured in the SGZ. Magnification, ×400; *bar* 50 μm

number was normalized with the length of the SGZ measured in female pups culled on PND 4.

A profile counting method was applied using 3 brain sections at approximately 250-μm intervals for the measurement of cellular distribution of immunoreactive cells and apoptotic bodies in pups or dams with animal groups and items listed in Table 1. Positive cells were counted in one brain section per animal when TUNEL-assay was performed on pups at PND 21 and in those used for immunohistochemistry of neuronal stage-defining markers on pups at PND 77.

For quantitative measurement of cells positive for immunohistochemistry or TUNEL-assay and apoptotic bodies, digital photomicrographs at 200× or 400× magnification were taken using a BX51 microscope (Olympus Optical Co., Ltd., Tokyo, Japan) attached to a DP70 Digital Camera System (Olympus Optical Co.), and quantitative measurements were performed using the WinROOF image analysis software package (Version 5.7, Mitani Corp., Fukui, Japan). Where the profile counting method was applied, the normalized number of positive cells or apoptotic bodies was averaged across the number of sections.

Real-time RT-PCR analysis

Transcript levels for genes listed in Online Resource 1 (Table s1) were analyzed with real-time RT-PCR in hippocampal tissues on PND 21. From total RNA samples extracted with RNeasy Mini Kit (QIAGEN, Hilden, Germany), first-strand cDNA was synthesized using SuperScript™ III Reverse Transcriptase (Invitrogen Corp., Carlsbad, CA, USA), and then real-time PCR analysis was performed using the SYBR®Green PCR Master Mix (Applied Biosystems Inc., Foster City, CA, USA) and the StepOnePlus™ Real-Time PCR System (Applied Biosystems Inc.). The PCR primers were designed for each gene using Primer Express software (Version 3.0; Applied Biosystems Inc.). The relative differences in gene expression was calculated using threshold cycle (C_T) values that were first normalized to those of the housekeeping gene, beta actin (*Actb*), or glyceraldehyde-3-phosphate dehydrogenase (*Gapdh*), as a endogenous control in the same sample, and then relative to a control C_T value by the $2^{-\Delta\Delta C_T}$ method (Livak and Schmittgen 2001).

Statistical analysis

Maternal data regarding the body weight and food consumption during the animal study as well as immunoreactive cell counts in the Experiment 1 were analyzed using the individual animal as the experimental unit. Data for offspring regarding the body and organ weights at necropsy in both the Experiment 1 and Experiment 2 were analyzed using the litter as the experimental unit. With regard to the data for cell counts immunoreactive for each antigen or apoptotic cells and real-time RT-PCR of pups, the individual animal was examined as the experimental unit.

For comparison of numerical data between the 0 ppm (control) and AA-dosed groups in Experiment 1, data were analyzed by the Bartlett's test for the homogeneity of variance. If there is no significant difference in variance, Dunnett's test was performed for comparison between the groups. If a significant difference was found in variance, Steel's test was then performed.

In case of numerical data consisting of two sample groups, data were analyzed by the F test for the homogeneity of variance and Student's t test was applied when the variance was homogenous among the groups using a test for equal variance. If a significant difference was observed in variance, Aspin–Welch's t test was used instead.

As for gait score data, Mann–Whitney's U test was used to compare between the untreated controls and AA-dosed animals.

Results

Maternal and reproductive parameters (Experiment 1)

There was no observable gait abnormality of dams through to the day 21 after delivery. There was one animal that was judged to be non-pregnant in the 100 ppm group by the examination of uterine implantation sites, and therefore, this animal was excluded from the experiment. No significant changes were observed in food intake and water consumption during the whole exposure period as compared with the 0 ppm controls (Online Resource 1, Table s2). At the necropsy on day 21 after delivery, a slight reduction in the absolute liver weight was observed at 100 ppm as compared with the 0 ppm controls (Online Resource 1, Table s2). Maternal exposure to AA did not affect the duration of pregnancy, number of implantation sites, live birth ratio, or male pup ratio.

In life changes and necropsy data of offspring

In Experiment 1, deaths of offspring were sporadically found in 0, 4, 20 ppm groups during PND 7–15; however, no other apparent abnormalities were found on clinical observation until weaning on PND 21. At the necropsy on PND 21, statistically significant decreases were found in the body and absolute brain weights of offspring at 100 ppm that continued to PND 77 (Online Resource 2, Fig. s1); however, any gait abnormalities were not observed from PND 21 to PND 77.

In Experiment 2, gait abnormalities were detected on most pups given AA directly showing statistically significant difference in the score from PND 15 as compared to the saline controls (Online Resource 2, Fig. s2). From PND 28, gradual recovery from gait abnormalities was observed in AA-injected animals, and any statistically significant difference was not observed in the score from PND 63. The body and absolute brain weights of AA-injected pups were significantly lower than those of saline controls at both PND 21 and PND 77 (Online Resource 2, Fig. s1).

Reelin- or NeuN-positive neurons in the dentate hilus

Distribution patterns of reelin- or NeuN-positive neurons in the hippocampus on both PND 21 and PND 77 were described previously (Saegusa et al. 2010; Ohishi et al. 2010). On PND 4, reelin-positive cells within the dentate gyrus were predominantly distributed in the molecular layer rather than the hilar region.

In Experiment 1, an increased density of reelin-positive cells and NeuN-positive cells in the hilus was observed with dose relation to AA from 20 ppm showing a statistically significant difference at 100 ppm on PND 21 (Fig. 2). On PND 77, no changes were observed in the density of reelin-positive cells with AA-exposure at any dose, but a significant increase in NeuN-positive cells was observed with AA from 20 ppm. We additionally examined reelin-positive cells in culled female pups on PND 4; however, there were no changes in positive cell distribution in either the molecular layer or the hilus (Online Resource 2, Fig. s3).

In Experiment 2, a significantly increased density of reelin-positive cells and NeuN-positive cells was observed in the hilus of AA-injected pups on PND 21, as compared with the saline controls (Fig. 2). On PND 77, no changes in the density of reelin-positive cells were observed with AA-injections; however, a significantly increased density of NeuN-positive cells in AA-injected pups was observed as compared to saline controls.

Proliferating and apoptotic cell counts at the SGZ

On PND 21, both PCNA-positive proliferating cells and Cresyl Violet-positive apoptotic bodies were observed in the SGZ similarly to the previous report (Fig. 3; Saegusa et al. 2010). On PND 77, however, numbers of both PCNA-positive cells and apoptotic bodies were rather decreased, and apoptotic bodies were not detected in many animals.

In Experiment 1, dose-dependent decrease in PCNA-positive cells was observed with AA-exposure on PND 21 with statistically significant difference from 20 ppm as compared with 0 ppm control (Fig. 3). There were no significant changes in the number of apoptotic bodies after AA-exposure (Fig. 3). Similarly, no significant decrease in TUNEL-positive cells was found after AA-exposure (Online Resource 2, Fig. s4). On PND 77, no changes in the number of PCNA-positive cells and apoptotic bodies were observed with AA at any dose (Fig. 3).

As in Experiment 1, a significant decrease in the number of PCNA-positive cells was found with direct AA-injections as compared with saline controls on PND 21 in Experiment 2 (Fig. 3); however, the number of apoptotic bodies was unchanged with AA-injections. On PND 77, the number of PCNA-positive cells or apoptotic bodies was not changed following AA-injections.

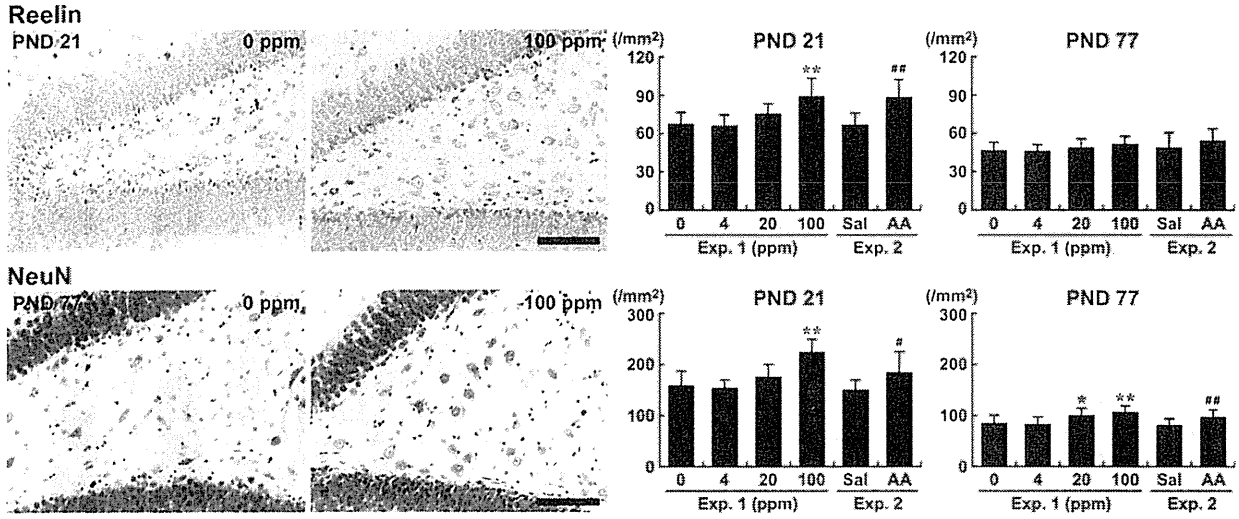

Fig. 2 Distribution of reelin- and NeuN-immunoreactive cells in the dentate hilus of male pups after AA-exposure. Photomicrographs are from Experiment 1. (*Left panels*) 0 ppm AA. (*Right panels*) 100 ppm AA. Magnification, ×200; *bar* 100 μm. The graphs show the density of reelin- or NeuN-positive cells in the hilus (bilateral) estimated applying a profile counting method. $N = 12$ (0 ppm controls), 11 (4 ppm), 11 (20 ppm), and 10 (100 ppm) in Experiment 1, and 12 (saline controls) and 12 (AA-injected animals) in Experiment 2 on PND 21. $N = 12$ (0 ppm controls), 12 (4 ppm), 12 (20 ppm), and 11 (100 ppm) in Experiment 1, and 12 (saline controls) and 12 (AA-injected animals) in Experiment 2 on PND 77. Values are expressed as mean + SD. $^{*}P < 0.05$; $^{**}P < 0.01$ versus 0 ppm control group (0 ppm) in Experiment 1 (Dunnett's or Steel's test). $^{\#}P < 0.05$; $^{\#\#}P < 0.01$ versus saline control group (vehicle saline) in Experiment 2 (Student's or Aspin–Welch's *t* test)

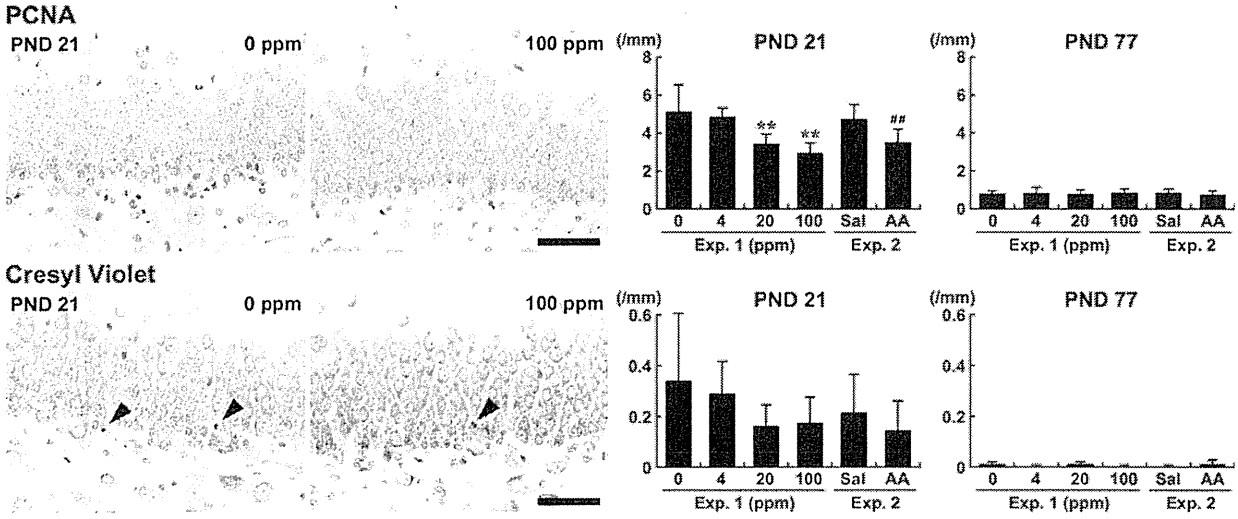

Fig. 3 Distribution of PCNA-immunoreactive proliferating cells and Cresyl Violet-positive apoptotic bodies (*arrowheads*) in the SGZ of male pups after AA-exposure. Photomicrographs are from Experiment 1. (*Left panels*) 0 ppm AA. (*Right panels*) 100 ppm AA. Magnification, ×200; *bar* 100 μm. The graphs show the number of PCNA-immunoreactive cells or apoptotic bodies in the SGZ (bilateral) estimated applying a profile counting method. Values are expressed as mean + SD. Numbers of animals examined in each group were identical to those in the analysis of reelin- or NeuN-immunoreactive cells shown in Fig. 2. $^{**}P < 0.01$ versus 0 ppm control group (0 ppm) in Experiment 1 (Dunnett's or Steel's test). $^{\#\#}P < 0.01$ versus saline control group (vehicle saline) in Experiment 2 (Student's or Aspin–Welch's *t* test)

Neuronal progenitor cells in the SGZ (Experiment 1)

On PND 21, statistically significant decreases in the number of Dpysl3- or Dcx-positive cells was found with AA-exposure as examined at 100 ppm as compared with 0 ppm controls (Fig. 4). However, there were no changes in the number of NeuroD1-, Tbr2- or Pax6-positive cells with AA at 100 ppm. By PND 77, no changes in the

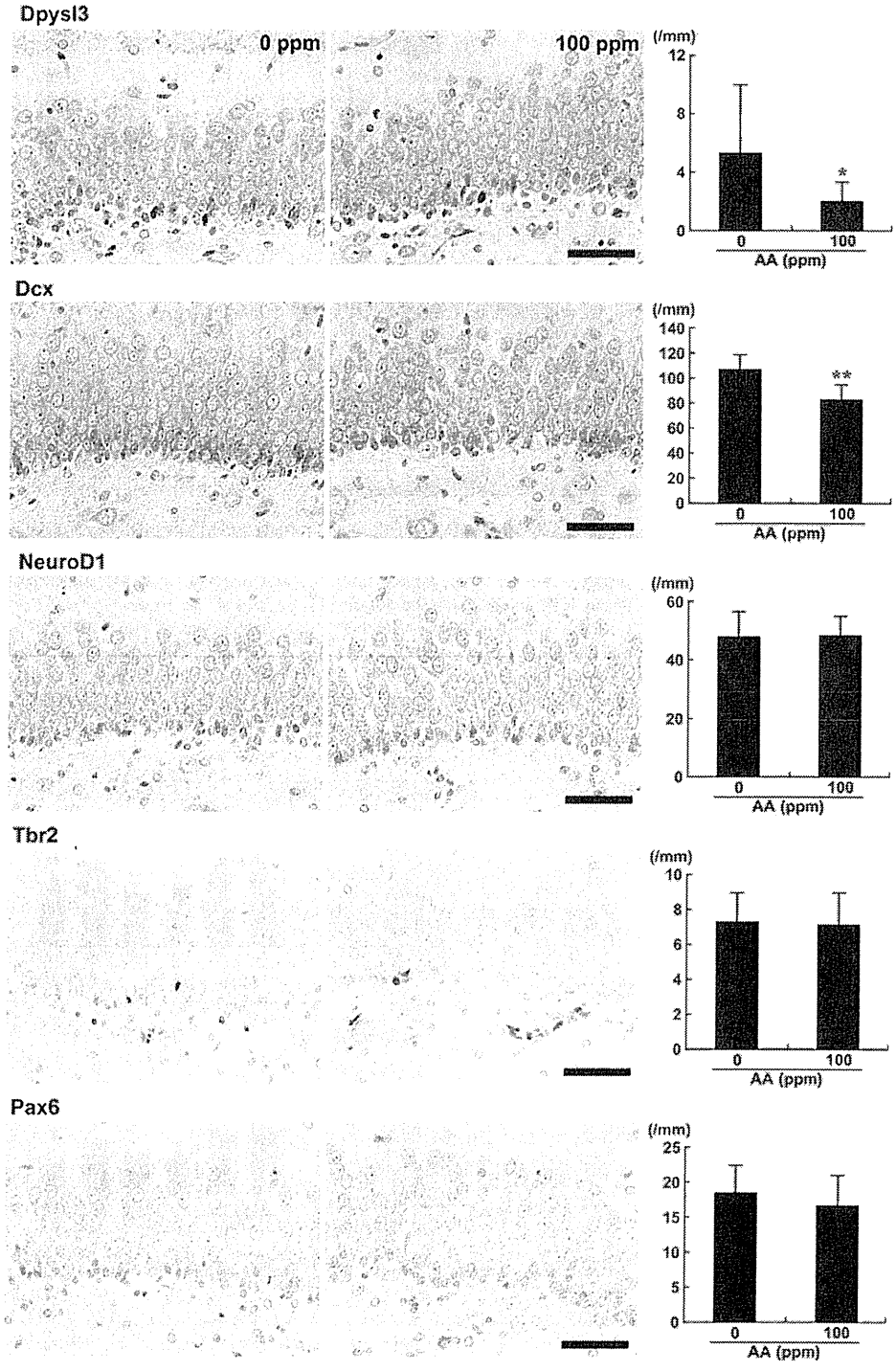

Fig. 4 Distribution of immunoreactive cells for neuronal stage-defining markers in the SGZ of male pups after AA-exposure examined on PND 21 in Experiment 1. (*Left panels*) 0 ppm AA. (*Right panels*) 100 ppm AA. Magnification, ×400; *bar* 50 μm. The graphs show the number of immunoreactive cells for each marker in the SGZ (bilateral) estimated applying a profile counting method. Values are expressed as mean + SD. $N = 12$ (0 ppm controls) and 10 (100 ppm). $^{*}P < 0.05$; $^{**}P < 0.01$ versus 0 ppm control group (0 ppm) (Student's or Aspin–Welch's *t* test)

number of Dpysl3- or Dcx-positive cells was observed with AA at 100 ppm (Online Resource 2, Fig. s5), while the numbers of immunoreactive cells were rather fewer than those at PND 21.

Dentate hilar area and length of the SGZ

In Experiment 1, a statistically significant decrease in the hilar area was found at 100 ppm as compared with 0 ppm

controls on PND 21 (Online Resource 2, Fig. s6). By PND 77, hilar area did not change after AA-exposure. There were no dose-related fluctuations in the length of SGZ at both PND 21 and PND 77, but a statistically significant increase was found at 4 and 20 ppm as compared with 0 ppm controls.

In Experiment 2, a statistically significant reduction was found in the hilar area by AA-injections as compared with the saline controls at both PND 21 and PND 77; however, there were no statistically significant difference in the SGZ-length at either PND 21 or PND 77 (Online Resource 2, Fig. s6).

Real-time RT-PCR data

There were no genes showing statistically significant up- or down-regulation more than one and half times the transcript levels between the AA-dosed animals and the corresponding controls commonly in both Experiment 1 and Experiment 2 (Online Resource 2, Fig. s7, s8). Also, there were no genes showing statistically significant fluctuations commonly in the values with the *Actb* and *Gapdh* normalizations in both Experiment 1 and Experiment 2 except for a slight upregulation of *Neurod1* transcript levels by both normalizations in Experiment 2.

Reelin- or PCNA-positive cells of dams

In dams of Experiment 1, there were no changes in the density of reelin-immunoreactive cells in the hilus or in the distribution of PCNA-positive cells in the SGZ with AA at 100 ppm (Fig. 5).

Discussion

In the present study, we detected an increased density of reelin-expressing interneurons in the hilus at 100 ppm and a decrease in PCNA-positive (i.e., proliferating) progenitor cells in the SGZ from 20 ppm in male offspring examined on PND 21, similar to the directly AA-injected cases. These results reproduce those in our recent study on weaning as found in male offspring (Ogawa et al. 2011). In the present study, we also observed a decrease in the hilar area at 100 ppm on PND 21, suggesting that the high density of reelin-producing interneurons in this group may be due to the reduction in the hilar volume. Because reelin is a large glycoprotein secreted to function as a ligand locally for the correct positioning of neurons (Rice and Curran 2001), cellular density rather than total cell number may be critical for exerting the local function of reelin. We have already shown decreased apoptotic bodies in the SGZ with AA at 100 ppm on PND 21 (Ogawa et al. 2011) but we did not detect apparent decrease in apoptotic bodies and TUNEL-positive cells after AA-exposure in the present study. We think that the shorter exposure period (GD 10–PND 21) in this study compared with that of the previous study (GD 6–PND 21) could explain the difference.

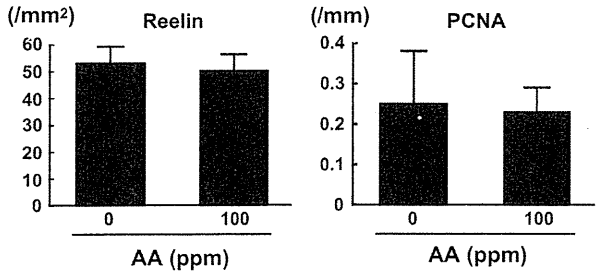

Fig. 5 Density of immunoreactive cells for reelin in the hilus and PCNA in the SGZ of dams in Experiment 1. The graphs show the density of reelin-immunoreactive cells in the hilus (bilateral) or the number of PCNA-positive cells in the SGZ (bilateral) estimated applying a profile counting method. Values are expressed as mean + SD. $N = 6$ (0 ppm controls) and 5 (100 ppm)

In the developmental exposure study of anti-thyroid agents in rats, we have previously observed sustained increase in reelin-positive and NeuN-negative immature interneurons in the dentate hilus on PND 77, as well as the increase in reelin-negative and NeuN-positive mature neurons (Saegusa et al. 2010). This result suggests that developmental hypothyroidism caused sustained impairment of neurogenesis and neuronal mismigration. In contrast, the distribution changes of reelin- and PCNA-positive cells at PND 21 in our AA-exposed cases here disappeared at PND 77, as with the recovery in the distribution of target progenitor cells, suggestive of a weak and reversible influence of AA on neurogenesis itself. Because reelin plays a role for repositioning of fully differentiated neurons to stabilize mature neuron circuitry (Frotscher 2010), no excess population of reelin-expressing cells at later stages observed here could be the reflection of no effect on the maintenance of neuron circuitry of migrated granule cells. Considering no effect on the mRNA expression levels in the hippocampus, in terms of reelin and related molecules, neuronal stage-defining marker molecules, cell proliferation marker molecule, and epigenetic event-related enzymes, observed cellular distribution changes on PND 21 by AA may be subtle and gradually progressive ones. However, no changes in the distribution of reelin- and PCNA-positive cells in dams suggest that offspring neurogenesis is much more sensitive to AA than the adult animals through maternal exposure.

In the present study, we found a sustained increase in cellular density of NeuN-positive mature neurons in the hilus after cessation of maternal exposure to AA from 20 ppm as well as ip-injected cases, while the reelin-positive population returned to the control level. In the

rodent dentate hilus, there are approximately equal numbers of GABAergic interneurons and other neurons (Houser 2007). We have found an increase in glutamic acid decarboxylase (GAD) 67-immunoreactive cells on PND 21 after maternal AA-exposure, confirming an increase in GABAergic interneurons (Ogawa et al. 2011). In the hypothyroidism model (Saegusa et al. 2010), we have found an increase in GAD67-positive population only at the adult stage, and the calbindin-D-28K-expressing population increased at the end of exposure on weaning. These results suggest that there are heterogeneous populations of interneurons showing different cellular potency depending on the type or magnitude of the insult on neurogenesis. We have recently found a transient increase in the density of reelin-producing interneurons associated with a sustained increase in mature neurons in the hilus by developmental exposure to brominated flame retardants (Saegusa et al., data submitted). However, we could not find fluctuations in the GAD67-positive populations either at the end of exposure or at the adult stage by these compounds. Because reelin is an inducible molecule and its expression level can be modified during the disease process (Kundakovic et al. 2009), it may be reasonable to consider that the excess population of reelin-producing interneurons during the AA-exposure halted their reelin production thereafter, reflecting a recovery from the effect on neurogenesis. Alternatively, the sustained increase in interneurons may be the signature of impaired neurogenesis during the developmental stages.

With regard to distribution changes in the neuronal progenitor cells in the SGZ, we revealed here decreases in Dcx- and Dpysl3-positive cells with 100 ppm AA on PND 21, while the distribution of progenitor cells expressing Pax6, Tbr2 and NuroD1 were unchanged. Pax6 and Tbr2 are markers for earlier stage progenitor cells (Breunig et al. 2007; Hodge et al. 2008). In contrast, NeuroD1 and Dcx are not neurogenesis markers with high specificity and are expressed from type-2b progenitor cells to immature granule cells with peak expression in type-3 cells and immature granule cells, respectively (Breunig et al. 2007; Hodge et al. 2008; Knoth et al. 2010). Dpysl3 is an early postmitotic neuronal marker of immature granule cells (Knoth et al. 2010). Therefore, we consider the decreased Dpysl3 by 100 ppm AA reported here represents immature granule cells. These cells already have both dendritic growth cones and recurrent basal dendrites, suggesting an entry into the process of synaptogenesis (Ribak et al. 2004). It is well known that AA targets nerve terminals due to impairment of neurotransmission by affecting diverse nerve terminal processes (Lopachin et al. 2008), suggesting the possibility of direct injury of immature granule cells by affecting the newly generating nerve terminals. However, we did not observe increase in apoptosis. Importantly, we observed suppression of progenitor cell proliferation by AA in the present study. Because immature granule cells can no longer proliferate, AA may rather target earlier type-3 progenitor cells to suppress their proliferation causing a reduction in immature granule cells.

We have shown that high doses of AA by direct ip-injections during the lactation period are necessary to induce an increase in reelin-producing interneurons, in contrast to the much lower doses to stimulate reelin expression if administered maternally from the gestation period onwards (Ogawa et al. 2011). We reproduced that result in this study. In humans, the internal level of AA in neonates by transplacental exposure was estimated to be at least equal to that of the mother (Schettgen et al. 2004). Considering that only about a tenth of maternal AA is transferred to offspring through lactation (Takahashi et al. 2009), transplacental rather than lactational transfer of AA may be responsible for the disruption of neurogenesis. On the other hand, in this study, we found that the number of reelin-positive cells distributed in the hilus and the molecular layer of the dentate gyrus, the former being interneurons and the latter Cajal–Retzius cells (Nakajima et al. 1997), was unchanged by maternal exposure to AA in culled pups on PND 4. Considering the immaturity of the postnatal "adult neurogenesis" in the dentate gyrus, target cell toxicity in the SGZ or responses of reelin-producing neurons would not appear at this time point. Although the putative mechanism of AA-action, whether through its known genotoxic potential or unknown epigenetic modification, should further be addressed, these results suggest a late onset for inducing aberrant neurogenesis after transplacental AA-exposure.

Epidemiological studies of human industrial and accidental exposures suggest that the nervous system is a principal site for toxicity in humans. At the sixty-fourth meeting of the Joint FAO/WHO Expert Committee on Food Additives, the committee concluded that based on national estimates, an intake of 0.001 mg/kg body weight/day of AA could be taken to represent the average for the general population and that an intake of 0.004 mg/kg body weight/day could be taken to represent high consumers (WHO/IPCS 2006). The committee also concluded that the non-observed effect level (NOEL) was determined to be 0.2 mg/kg body weight/day for the induction of distal axonopathy detected using electron microscopy in rats exposed to AA in drinking water for 90 days (Burek et al. 1980). The overall NOEL for reproductive and developmental effects and other non-neoplastic lesions was determined as 2 mg/kg body weight/day (Tyl et al. 2000). Based on the calculated margins of exposure, the committee concluded that adverse effects based on these endpoints are unlikely at the estimated average intakes, but that distal axonopathy changes cannot be excluded for some individuals with very high intake (WHO/IPCS 2006). In the

present study, the mild but sustained increase in mature neurons in the hilus from 20 ppm was considered to be irreversible, and thus, 4 ppm was determined to be the non-observed adverse effect level (NOAEL), translating into 0.36–0.89 mg/kg body weight/day. Considering the intake values for infants and children as 2–3 times higher than for adults when expressed on a body weight basis (WHO/IPCS 2006), the effect level in our present study may be equivalent to that detecting distal axonopathy by Burek et al. (1980). Nonetheless, administered AA is mutagenic and acts as a genotoxic carcinogen targeting multiple organs in rats (Rice 2005), and appropriate efforts to reduce AA concentrations in foodstuffs should continue as concluded by the Committee above mentioned (WHO/IPCS 2006).

In conclusion, while the neurotoxic effect of AA on neurogenesis and following neuronal migration in the dentate gyrus observed from 20 ppm was subtle and reversible, the sustained increase in mature neurons in the hilus at the later stages after AA-exposure from 20 ppm was considered to be irreversible. Because dysfunctional GABAergic interneurons are central contributors to a number of diseases such as schizophrenia and epilepsy (Dudek and Sutula 2007; Jones 2010), the biological significance of the excess population of inhibitory interneurons by AA on the neural circuits should further be assessed with regard to functional endpoints of the hippocampal dentate gyrus on learning, memory, and motivation.

Acknowledgments The authors thank Mrs. Shigeko Suzuki for her technical assistance in preparing the histological specimens. This work was supported by Health and Labour Sciences Research Grants (Research on Risk of Chemical Substances) from the Ministry of Health, Labour and Welfare of Japan. All authors disclose that there are no conflicts of interest that could inappropriately influence the outcome of the present study.

References

Breunig JJ, Silbereis J, Vaccarino FM, Sestan N, Rakic P (2007) Notch regulates cell fate and dendrite morphology of newborn neurons in the postnatal dentate gyrus. Proc Natl Acad Sci USA 104:20558–20563

Burek JD, Albee RR, Beyer JE, Bell TJ, Carreon RM, Morden DC, Wade CE, Hermann EA, Gorzinski SJ (1980) Subchronic toxicity of acrylamide administered to rats in the drinking water followed by up to 144 days of recovery. J Environ Pathol Toxicol 4:157–182

Choi JH, Yoo KY, Lee CH, Yi SS, Yoo DY, Seong JK, Yoon YS, Hwang IK, Won MH (2011) Effects of treadmill exercise combined with MK 801 treatment on neuroblast differentiation in the dentate gyrus in rats. Cell Mol Neurobiol 31:285–292

Dudek FE, Sutula TP (2007) Epileptogenesis in the dentate gyrus: a critical perspective. Prog Brain Res 163:755–773

Exon JH (2006) A review of the toxicology of acrylamide. J Toxicol Environ Health B Crit Rev 9:397–412

Friedman MA, Tyl RW, Marr MC, Myers CB, Gerling FS, Ross WP (1999) Effects of lactational administration of acrylamide on rat dams and offspring. Reprod Toxicol 13:511–520

Frotscher M (2010) Role for reelin in stabilizing cortical architecture. Trends Neurosci 33:407–414

Hodge RD, Kowalczyk TD, Wolf SA, Encinas JM, Rippey C, Enikolopov G, Kempermann G, Hevner RF (2008) Intermediate progenitors in adult hippocampal neurogenesis: Tbr2 expression and coordinate regulation of neuronal output. J Neurosci 28:3707–3717

Houser CR (2007) Interneurons of the dentate gyrus: an overview of cell types, terminal fields and neurochemical identity. Prog Brain Res 163:217–232

Hwang IK, Yoo KY, Yoo DY, Choi JH, Lee CH, Kang IJ, Kwon DY, Kim YS, Kim DW, Won MH (2011) Zizyphus enhances cell proliferation and neuroblast differentiation in the subgranular zone of the dentate gyrus in middle-aged mice. J Med Food 14:195–200

Jones MW (2010) Errant ensembles: dysfunctional neuronal network dynamics in schizophrenia. Biochem Soc Trans 38:516–521

Knoth R, Singec I, Ditter M, Pantazis G, Capetian P, Meyer RP, Horvat V, Volk B, Kempermann G (2010) Murine features of neurogenesis in the human hippocampus across the lifespan from 0 to 100 years. PLoS One 5:e8809

Kundakovic M, Chen Y, Guidotti A, Grayson DR (2009) The reelin and GAD67 promoters are activated by epigenetic drugs that facilitate the disruption of local repressor complexes. Mol Pharmacol 75:342–354

Lee K-Y, Shibutani M, Kuroiwa K, Takagi H, Inoue K, Nishikawa H, Miki T, Hirose M (2005) Chemoprevention of acrylamide toxicity by antioxidative agents in rats—effective suppression of testicular toxicity by phenylethyl isothiocyanate. Arch Toxicol 79:531–541

Lee K-Y, Shibutani M, Inoue K, Kuroiwa K, Mami U, Woo G-H, Hirose M (2006) Methacarn fixation—effects of tissue processing and storage conditions on detection of mRNAs and proteins in paraffin-embedded tissues. Anal Biochem 351:36–43

Livak KJ, Schmittgen TD (2001) Analysis of relative gene expression data using real-time quantitative PCR and the $2^{-\Delta\Delta C_T}$ method. Methods 25:402–408

LoPachin RM (2004) The changing view of acrylamide neurotoxicity. NeuroToxicology 25:617–630

LoPachin RM, Barber DS, Gavin T (2008) Molecular mechanisms of the conjugated alpha, beta-unsaturated carbonyl derivatives: relevance to neurotoxicity and neurodegenerative diseases. Toxicol Sci 104:235–249

Lussier AL, Caruncho HJ, Kalynchuk LE (2009) Repeated exposure to corticosterone, but not restraint, decreases the number of reelin-positive cells in the adult rat hippocampus. Neurosci Lett 460:170–174

Mottram DS, Wedzicha BL, Dodson AT (2002) Acrylamide is formed in the Maillard reaction. Nature 419:448–449

Nakajima K, Mikoshiba K, Miyata T, Kudo C, Ogawa M (1997) Disruption of hippocampal development in vivo by CR-50 mAb against reelin. Proc Natl Acad Sci USA 94:8196–8201

Nam SM, Yoo DY, Kim W, Yoo M, Kim DW, Won MH, Hwang IK, Yoon YS (2011) Effects of *S*-allyl-L-cysteine on cell proliferation and neuroblast differentiation in the mouse dentate gyrus. J Vet Med Sci 73:1071–1075

Nóbrega-Pereira S, Marín O (2009) Transcriptional control of neuronal migration in the developing mouse brain. Cereb Cortex 19(Suppl 1):i107–i113

Nuñez JL, McCarthy MM (2004) Cell death in the rat hippocampus in a model of prenatal brain injury: time course and expression of death-related proteins. Neuroscience 129:393–402

Ogawa B, Ohishi T, Wang L, Takahashi M, Taniai E, Hayashi H, Mitsumori K, Shibutani M (2011) Disruptive neuronal development by acrylamide in the hippocampal dentate hilus after developmental exposure in rats. Arch Toxicol. doi:10.1007/s00204-010-0622-9 (Online 1 Dec 2010)

Ohishi T, Wang L, Ogawa B, Fujisawa K, Taniai E, Hayashi H, Mitsumori K, Shibutani M (2010) No effect of sustained systemic growth retardation on the distribution of reelin-expressing interneurons in the neuron-producing hippocampal dentate gyrus in rats. Reprod Toxicol 30:591–599

Ribak CE, Korn MJ, Shan Z, Obenaus A (2004) Dendritic growth cones and recurrent basal dendrites are typical features of newly generated dentate granule cells in the adult hippocampus. Brain Res 1000:195–199

Rice JM (2005) The carcinogenicity of acrylamide. Mutat Res 580:3–20

Rice DS, Curran T (2001) Role of the reelin signaling pathway in central nervous system development. Annu Rev Neurosci 24:1005–1039

Saegusa Y, Woo G-H, Fujimoto H, Kemmochi S, Shimamoto K, Mitsumori K, Nishikawa A, Shibutani M (2010) Sustained production of reelin-expressing interneurons in the hippocampal dentate hilus after developmental exposure to anti-thyroid agents in rats. Reprod Toxicol 29:407–414

Saita K, Ohi T, Hanaoka Y, Furukawa S, Furukawa Y, Hayashi K, Matsukura S (1996) A catechol derivative (4-methylcatechol) accelerates the recovery from experimental acrylamide-induced neuropathy. J Pharmacol Exp Ther 276:231–237

Schettgen T, Kütting B, Hornig M, Beckmann MW, Weiss T, Drexler H, Angerer J (2004) Trans-placental exposure of neonates to acrylamide—a pilot study. Int Arch Occup Environ Health 77:213–216

Takahashi M, Shibutani M, Nakahigashi J, Sakaguchi N, Inoue K, Morikawa T, Yoshida M, Nishikawa A (2009) Limited lactational transfer of acrylamide to rat offspring on maternal oral administration during the gestation and lactation periods. Arch Toxicol 83:785–793

Tyl RW, Friedman MA, Losco PE, Fisher LC, Johnson KA, Strother DE, Wolf CH (2000) Rat two-generation reproduction and dominant lethal study of acrylamide in drinking water. Reprod Toxicol 14:385–401

WHO/IPCS (2006) Summary and conclusions of the sixty-fourth meeting of the Joint FAO/WHO Expert Committee on Food Additives (JECFA), Rome, 8–17 Feb 2005. Available from: http://www.who.int/ipcs/food/jecfa/summaries/summary_report_64_final.pdf

Yan BC, Yoo KY, Park JH, Lee CH, Choi JH, Won MH (2011) The high dosage of earthworm (*Eisenia andrei*) extract decreases cell proliferation and neuroblast differentiation in the mouse hippocampal dentate gyrus. Anat Cell Biol 44:218–225

Yoo DY, Kim W, Kim DW, Yoo KY, Chung JY, Youn HY, Yoon YS, Choi SY, Won MH, Hwang IK (2011) Pyridoxine enhances cell proliferation and neuroblast differentiation by upregulating the GABAergic system in the mouse dentate gyrus. Neurochem Res 36:713–721

Zhang L, Blomgren K, Kuhn HG, Cooper-Kuhn CM (2009) Effects of postnatal thyroid hormone deficiency on neurogenesis in the juvenile and adult rat. Neurobiol Dis 34:366–374

Arch Toxicol
DOI 10.1007/s00204-012-0824-4

REPRODUCTIVE TOXICOLOGY

Transient aberration of neuronal development in the hippocampal dentate gyrus after developmental exposure to brominated flame retardants in rats

Yukie Saegusa · Hitoshi Fujimoto · Gye-Hyeong Woo · Takumi Ohishi · Liyun Wang · Kunitoshi Mitsumori · Akiyoshi Nishikawa · Makoto Shibutani

Received: 29 September 2011 / Accepted: 27 February 2012

Abstract We immunohistochemically investigated the impact and reversibility of three brominated flame retardants (BFRs) known to be weak thyroid hormone disruptors on neuronal development in the hippocampal formation and apoptosis in the dentate subgranular zone. Pregnant Sprague–Dawley rats were exposed to 10, 100, or 1,000 ppm decabromodiphenyl ether (DBDE); 100, 1,000 or 10,000 ppm tetrabromobisphenol A (TBBPA) or 1,2,5,6,9,10-hexabromocyclododecane (HBCD) in the diet from gestational day 10 through to day 20 after delivery (weaning). On postnatal day (PND) 20, interneurons in the dentate hilus–expressing reelin increased with all chemicals, suggestive of aberration of neuronal migration. However, this increase had disappeared by PND 77. NeuN-positive mature neurons increased in the hilus on PND 77 with all chemicals. In the subgranular zone on PND 20, an increase in apoptotic bodies suggestive of impaired neurogenesis was observed after exposure to TBBPA or HBCD. The effects on neuronal development were detected at doses of ≥100 ppm DBDE; ≥1,000 ppm TBBPA; and at least at 10,000 ppm HBCD. On PND 20, the highest dose of DBDE and HBCD revealed mild fluctuations in the serum concentrations of thyroid-related hormones suggestive of weak developmental hypothyroidism, while TBBPA did not. Thus, DBDE and TBBPA may exert direct effect on neuronal development in the brain, but hypothyroidism may be operated for DBDE and HBCD at high doses. An excess of mature neurons in the hilus at later stages may be the signature of the developmental effects of BFRs. However, the effect itself was reversible.

Keywords Reelin · Brominated flame retardants · Hippocampal dentate gyrus · Hypothyroidism · Neurogenesis · Neuronal migration

Abbreviations

BFRs	Brominated flame retardants
BW	Body weight
CA1	Cornu ammonis 1
DBDE	Decabromodiphenyl ether
EphA5	Ephrin type A receptor 5
GABA	γ-Aminobutyric acid
GAD67	Glutamic acid decarboxylase 67
GD	Gestational day
HBCD	1,2,5,6,9,10-Hexabromocyclododecane
NeuN	Neuron-specific nuclear protein
PND	Postnatal day
SGZ	Subgranular zone
Tacr3	Tachykinin receptor 3

Electronic supplementary material The online version of this article (doi:10.1007/s00204-012-0824-4) contains supplementary material, which is available to authorized users.

Y. Saegusa · T. Ohishi · L. Wang · K. Mitsumori · M. Shibutani (✉)
Laboratory of Veterinary Pathology, Tokyo University of Agriculture and Technology, 3-5-8 Saiwai-cho, Fuchu-shi, Tokyo 183-8509, Japan
e-mail: mshibuta@cc.tuat.ac.jp

Y. Saegusa
Pathogenetic Veterinary Science, United Graduate School of Veterinary Sciences, Gifu University, 1-1 Yanagido, Gifu-shi, Gifu 501-1193, Japan

H. Fujimoto · G.-H. Woo · M. Shibutani
Division of Pathology, National Institute of Health Sciences, 1-18-1 Kamiyoga, Setagaya-ku, Tokyo 158-8501, Japan

A. Nishikawa
Biological Safety Research Center, National Institute of Health Sciences, 1-18-1 Kamiyoga, Setagaya-ku, Tokyo 158-8501, Japan

Published online: 14 March 2012

TBBPA	Tetrabromobisphenol A
TH	Thyroid hormone
T_3	Triiodothyronine
T_4	Thyroxine
TSH	Thyroid-stimulating hormone

Introduction

Thyroid hormones (THs) are essential for normal brain development in animals and humans. They regulate neuronal proliferation, migration, and differentiation in discrete regions of the brain during definitive time periods (Porterfield 2000). Experimentally, developmental hypothyroidism leads to growth retardation, neurological defects, and impaired performance in a variety of behavioral learning actions (Comer and Norton 1982; Akaike et al. 1991). Rat offspring exposed in utero to maternal antithyroid agents show impaired brain growth with neuronal mismigration and white matter hypoplasia involving limited axonal myelination and decreased oligodendroglial distribution (Lavado-Autric et al. 2003; Schoonover et al. 2004). The outcome of this type of impairment is permanent and is accompanied by apparent structural and functional abnormalities.

The dentate gyrus in the hippocampal formation is a unique structure that can continue neurogenesis during postnatal life and is a well-known target for developmental hypothyroidism (Zhang et al. 2009). By developmental hypothyroidism, we have recently detected an increase in reelin-expressing γ-aminobutyric acid (GABA)ergic interneurons showing immature phenotype in the dentate hilus that was sustained through to the adult stage, as well as increased apoptosis and decreased cell proliferation suggestive of impaired neurogenesis in the neuroblast-producing subgranular zone (SGZ; Saegusa et al. 2010b). Reelin is a secreted extracellular matrix glycoprotein that plays a critical role in neuronal migration and positioning during brain development (D'Arcangelo et al. 1997; Alvarez-Dolado et al. 1999). Also, it has been suggested that reelin release by GABAergic interneurons in adults could regulate the migration and maturation of newborn granular cells in the dentate granular cell layer (Lussier et al. 2009). Therefore, our observation of the sustained increase in reelin-producing immature GABAergic interneurons in the hilus suggests a compensatory regulation for neuronal mismigration that continues to the adult stage in relation with developmental hypothyroidism (Saegusa et al. 2010b). Altered reelin signaling has been reported in the dentate gyrus in some neurological diseases such as depression and epilepsy (Lussier et al. 2009; Gong et al. 2007).

In a study to establish a morphometric detection system of aberrant neuronal migration, we have shown fluctuations in the distribution of pyramidal neurons in the cornu ammonis 1 (CA1) of the hippocampus in a model for hypothyroidism induced by maternal administration of antithyroid agents in rats (Shibutani et al. 2009). Using this model, we also identified candidates for immunohistochemical molecular markers reflecting impaired neuronal development in the hippocampal formation, such as Ephrin type A receptor 5 (EphA5) and Tachykinin receptor (Tacr)-3, using microarray analysis (Saegusa et al. 2010a). EphA5 is a tyrosine kinase receptor that is particularly important in mediating neurodevelopmental events, such as neurogenesis, neuronal migration, and the plasticity (Numachi et al. 2007; Cooper et al. 2009). Tacr3 is a tachykinin peptide neurotransmitter/neuromodulator receptor predominantly expressed in neurons involving the hippocampus (Smith and Dawson 2008). It has been shown to play a role in the survival and function of dopaminergic neurons (Salthun-Lassalle et al. 2005). We have previously found an increase in both EphA5- and Tacr3-immunoreactive cells with strong intensities in the pyramidal cell layer or stratum oriens of the CA1 on weaning after developmental hypothyroidism, with a sustained increase in Tacr3-expressing cells through to the adult stage (Saegusa et al. 2010a).

Some environmental chemicals are thought to potentiate a TH–disrupting effect that may lead to abnormal brain development (Bansal and Zoeller 2008). Particularly, brominated flame retardants (BFRs), some of which are environmental contaminants used in plastics, textiles, electronic circuitry and other materials to prevent fires, are known to be the weak TH disruptors. Therefore, there is a growing concern regarding the developmental neurotoxicity of these chemicals (de Wit 2002; Rice et al. 2007). Decabromodiphenyl ether (DBDE), tetrabromobisphenol A (TBBPA), and 1,2,5,6,9,10-hexabromocyclododecane (HBCD) are three widely used BFRs (Birnbaum and Staskal 2004) that have been reported to cause neurobehavioral and auditory response effects by developmental exposure in mice and rats (Rice et al. 2007; Viberg et al. 2003, 2007; van der Ven et al. 2008; Lilienthal et al. 2008; Eriksson et al. 2006; Ema et al. 2008). These BFRs have shown weak antithyroid activities in some studies (Kitamura et al. 2005; Rice et al. 2007; Ema et al. 2008; Saegusa et al. 2009; Fujimoto et al. 2011). On the other hand, there are experimental studies to suggest direct effect on the developing brain by these BFRs (Nakajima et al. 2009; Ibhazehiebo et al. 2011a, b, c).

We have recently reported the effects of developmental exposure to DBDE, TBBPA, and HBCD on the migration of the hippocampal CA1 pyramidal cells and white matter

development by histomorphometric assessment using rats in association with thyroid parameters (Saegusa et al. 2009; Fujimoto et al. 2011). Our results suggested that maternal exposure to DBDE or HBCD through diet caused irreversible white matter hypoplasia at highest doses in offspring as examined in males, as well as the induction of mild developmental hypothyroidism as judged by fluctuations in the serum concentrations of thyroid-related hormones at the end of developmental exposure (Saegusa et al. 2009; Fujimoto et al. 2011; Online Resource 1, Table s1). However, no effect of BFR exposure could be detected on histologically observable neuronal migration. In the present study, we investigated the effects of these BFRs on neuronal development by analyzing cellular changes in the distribution of reelin in the dentate hilus and of EphA5 and Tacr3 in the CA1 region immediately after developmental exposure and at later stages for analysis of reversibility using the same study samples examined previously (Saegusa et al. 2009; Fujimoto et al. 2011). We also examined the effects on neurogenesis in the SGZ in terms of apoptosis at both time points.

Materials and methods

Chemicals and animals

Decabromodiphenyl ether (DBDE; CAS No. 1163–19–5, purity: >98%) was purchased from Wako Pure Chemical Industries, Ltd. (Osaka, Japan). Tetrabromobisphenol A (TBBPA; CAS No.79–94–7, purity: >98%) and 1,2,5,6,9,10-hexabromocyclododecane (HBCD; CAS No. 3194–55–6, purity: >95%) were purchased from Tokyo Kasei Kogyo Co., Ltd. (Tokyo, Japan). Pregnant Crj:CD® (SD)IGS rats were purchased from Charles River Japan Inc. (Yokohama, Japan) at gestational day (GD) 3 (appearance of vaginal plugs was designated as GD 0). Rats were housed individually in polycarbonate cages with wood chip bedding, maintained in an air-conditioned animal room (temperature 24 ± 1°C, relative humidity: 55 ± 5%) with a 12-h light/dark cycle and allowed ad libitum access to feed and tap water (Saegusa et al. 2009; Fujimoto et al. 2011). A soy-free diet (Oriental Yeast Co., Ltd., Tokyo, Japan) was chosen as the basal diet for the dams to eliminate possible phytoestrogen effects as described previously (Masutomi et al. 2003). All offspring consumed a regular CRF-1 basal diet (Oriental Yeast Co., Ltd.) and water ad libitum from postnatal day (PND) 20 onwards (PND 0 being the day of delivery). Although the formula is not public, CRF-1 contains soybean and alfalfa-derived proteins and oils including daidzin and genistin at concentrations of 87 and 102 ppm according to the supplier's analysis, and coumestrol of <3 ppm based on the content of lucerne meal in the diet (supplier's comment). The soy-free diet was prepared based on the formulation of the NIH-07 open formula rodent diet, in which soybean meal and soy oil were replaced with ground corn, ground wheat, wheat middlings and corn oil. Values for phytoestrogens in this diet were below the detection limit (0.5 ppm), except for coumestrol (3 ppm). Estrogen equivalents of phytoestrogens included in the CRF-1 and soy-free diet were roughly calculated as 0.91 and 0.06 ppm, respectively, for β-estradiol, based on the relative binding affinities in a rat endometrium-derived experimental model (Hopert et al. 1998). Nutritional standards did not differ between the soy-free diet and CRF-1 (supplier's analysis).

Animal experiments

Exposure studies to DBDE, HBCD, and TBBPA were individually performed, and dams were randomly divided into four groups including untreated controls (Saegusa et al. 2009; Fujimoto et al. 2011). The highest dose of each chemical was determined with a preliminary dose-finding study by estimating the dose range that causes changes in thyroid weights and histopathological findings of thyroid glands in dams, but does not affect pregnancy, implantation, or delivery. For DBDE, 8 dams per group were provided with the soy-free diet containing 0 (control), 10, 100, or 1,000 ppm of DBDE from GD 10 to day 20 after delivery. For TBBPA or HBCD, 8 dams per group in the TBBPA study and 10 dams per group in the HBCD study were provided with the soy-free diet containing 0 (control), 100, 1,000, or 10,000 ppm of the compound from GD 10 to day 20 after delivery. In all studies, litters were culled randomly on PND 2, leaving 4 male and 4 female offspring. On PND 20, 20 male and 20 female offspring (at least one male and one female per dam) per group were killed and subjected to prepubertal necropsy. Body and brain weights were measured for 10 male offspring at PND 20. The remaining animals were killed on PND 77 and subjected to adult stage necropsy. Body and brain weights were measured.

All animals used in the present study were killed by exsanguination from the abdominal aorta under deep anesthesia with ether. The protocols were reviewed in terms of animal welfare and approved by the Animal Care and Use Committee of the National Institute of Health Sciences, Japan.

As reported previously, no major treatment-related changes were observed in dams during gestation and lactation periods in all studies (Saegusa et al. 2009; Fujimoto et al. 2011; Online Resource 1, Table s2). At necropsy on day 20 after delivery, dose-unrelated increase in the relative thyroid weight was observed at 10 and 1,000 ppm in the DBDE study. In the TBBPA study, there were no

statistically significant changes in relative weight and histopathology of the thyroid on this time point. In the HBCD study, a significant increase in relative thyroid weights associated with significantly increased incidence and severity of diffuse thyroid follicular cell hypertrophy was observed at 10,000 ppm.

With regard to the body and organ weights of offspring as examined in males, no treatment-related changes in body and relative brain weights were observed on PND 20 in all studies (Fujimoto et al. 2011; Saegusa et al. 2009; Online Resource 1, Table s3). On PND 77, dose-unrelated increase in body weight and decrease in relative brain weights were observed at 10 and 100 ppm in the DBDE study, while relative thyroid weights were unchanged at any dose. In the TBBPA study, no treatment-related changes were observed in these parameters. In the HBCD study, a slight but significant dose-related increase was observed in relative thyroid weight from 1,000 ppm at this time point, while body and relative brain weights were unchanged.

Immunohistochemistry and Cresyl violet staining

For immunohistochemical studies, brains of male pups obtained at PND 20 or PND 77 were fixed in Bouin's solution at room temperature overnight. For analysis of PND 20 tissues, 5–6 animals (1 pup/litter) were examined per group including untreated controls in the DBDE study, 8 animals (1 pup/litter) were used per group in the TBBPA study, and 10 animals (1 pup/litter) per group in the HBCD study. For analysis of PND 77 tissues, 10 animals (1–2 pups/litter) were used from the untreated controls and the 10 ppm and 100 ppm DBDE exposure groups, and 11 (1–2 pups/litter) from the 1,000 ppm exposure group. In the TBBPA study, 10 animals (1–2 pups/litter) were used from the untreated controls and all exposure groups. In the HBCD study, 13 animals were used from the untreated controls, and 14 from the 100 ppm, 12 from the 1,000 ppm, and 14 from the 10,000 ppm exposure groups (1–2 pups/litter). Coronal slices were prepared from brains of PND 20 and PND 77 at the positions of −3.0 and −3.5 mm from the bregma, respectively.

Immunohistochemistry was performed on 3-μm brain tissue sections of animals killed at PND 20 and PND 77 with antibodies against reelin (clone G10, mouse IgG_1, 1:1,000; Novus Biologicals, Inc., Littleton, CO, United States), glutamic acid decarboxylase 67 (GAD67; clone 1G10.2, mouse IgG_{2a}, 1:50; Millipore Corporation Temecula, CA, United States), EphA5 (rabbit IgG, 1:50; Abcam, Cambridge, UK), and Tacr3 (rabbit polyclonal antibody, 1:3,000; Novus Biologicals, Inc.) as previously described (Saegusa et al. 2010a, b). Immunohistochemistry of neuron-specific nuclear protein (NeuN; clone A60, mouse IgG_1, 1:1,000; Millipore Corporation), which specifically detects postmitotic neurons, was performed on PND 77 brain sections (Saegusa et al. 2010b). Antigen retrieval treatment was not conducted for these antigens. Immunodetection was carried out using a VECTASTAIN® Elite ABC kit (Vector Laboratories Inc., Burlingame, CA, United States) with 3,3′-diaminobenzidine/H_2O_2 as the chromogen, as described previously (Saegusa et al. 2010a, b). The sections were then counterstained with hematoxylin and coverslipped for microscopic examination.

For evaluation of apoptosis in the hippocampal substructure, apoptotic bodies were detected by Cresyl violet staining as described by others (Nuñez and McCarthy 2004).

Morphometry of immunolocalized cells and apoptotic cells

Reelin-, NeuN-, or GAD67-positive cells distributed in the hilus of the dentate gyrus were bilaterally counted and averaged per mm^2 of hilar area (polymorphic layer) as described previously (Fig. 1; Saegusa et al. 2010b). EphA5- or Tacr3-immunoreactive cells distributed in the pyramidal cell layer or stratum oriens of the hippocampal CA1 region were bilaterally counted and normalized for

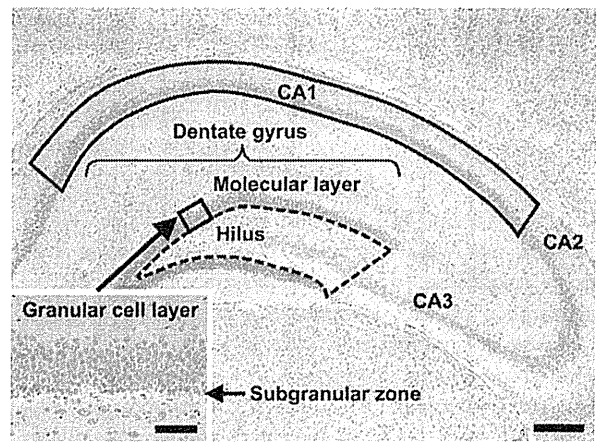

Fig. 1 Overview of the hippocampal formation of a male rat at PND 20 stained with hematoxylin and eosin. *Inset* shows a higher magnification of the granular cell layer and subgranular zone. *Bar* = 200 μm (*Inset*: 100 μm). Immunoreactive cells for reelin and GAD67 were counted in the hilus of the dentate gyrus, as enclosed by the *dotted line*, and averaged per area unit. Small-sized neurons in this area showed positive immunoreactivity with these antigens, but large-sized CA3 neurons distributed in this area were not immunoreactive. NeuN-immunoreactive cells were similarly counted and averaged per area unit, but CA3 neurons distributed in this area that were positive for NeuN were excluded from counting. The number of cells immunoreactive for EphA5 and Tacr3 in the area within the pyramidal cell layer and stratum oriens of the CA1 region, enclosed by a *solid line*, was normalized for the length of CA1 measured

the length of the CA1 region measured as previously described (Saegusa et al. 2010a). Apoptotic bodies detected by Cresyl violet staining were bilaterally counted and averaged per unit length of the SGZ as previously described (Saegusa et al. 2010b). For quantitative measurement of immunoreactive cells and apoptotic bodies, digital photomicrographs at 100-fold magnification were taken using a BX51 microscope (Olympus Optical Co., Ltd., Tokyo, Japan) attached to a DP70 Digital Camera System (Olympus Optical Co., Ltd.). Quantitative measurements were taken using the WinROOF image analysis software package (version 5.7, Mitani Corp., Fukui, Japan).

Statistical analysis

Numerical data were analyzed for homogeneity of variance using Bartlett's test. When the variance was homogeneous among the groups, a one-way analysis of variance was carried out. If significant differences were found, the mean value for each exposure group was compared with that of the controls using Dunnett's test. When the variance was heterogeneous based on Bartlett's test, the Kruskal–Wallis's H test was employed to check for differences among the groups. If significant differences appeared, a Dunnett-type rank-sum test was performed.

Results

Reelin-, NeuN-, and GAD67-immunoreactive cells in the hippocampal dentate hilus

The distribution of reelin-, NeuN-, and GAD67-immunoreactive cells in the hippocampal formation including the CA1–3 regions was similar to that described previously. Immunoreactive cells within the hilus of the dentate gyrus were predominantly interneurons (Saegusa et al. 2010b).

On PND 20, statistically significant dose-related increases in the number of reelin-immunoreactive cells were observed at 100 ppm and higher in the dentate hilus in both the DBDE and TBBPA studies (Fig. 2a). In the HBCD study, a statistically significant increase in the number of reelin-positive cells was observed at 1,000 ppm compared with the untreated controls on PND 20. However, the number at 10,000 ppm was not different from untreated controls. On PND 77, there were no effects of any of the BFRs on the number of reelin-positive cells in the hilus at any dose.

At PND 77, a weak but statistically significant increase in NeuN-immunoreactive cells was found in the hilus at 1,000 ppm in the DBDE study (Fig. 2b). In the TBBPA study, a slight dose-related increase in NeuN-positive cells was observed at 1,000 ppm and higher. In the HBCD study, a significant increase in NeuN-positive cells was observed at 10,000 ppm.

No changes were observed in the number of GAD67-immunoreactive cells in the highest dose groups compared with the untreated controls at both PND 20 and PND 77 in any of DBDE, TBBPA, and HBCD studies (Fig. 3).

EphA5- and Tacr3-immunoreactive cells in the hippocampal CA1 region

Both EphA5- and Tacr3-positive cells were sparse within the pyramidal cell layer or stratum oriens of the CA1 region, as shown in our previous study (Saegusa et al. 2010a).

With regard to EphA5-immunoreactivity, a significantly increased number of positive cells were observed only at 1,000 ppm on PND 20 in the DBDE study (Fig. 4a). There was no effect on the number of EphA5-positive cells in the TBBPA and HBCD studies at any dose at this time point. In the DBDE study, the number of EphA5-positive cells on PND 77 was unchanged at any dose, and the number of positive cells was low compared with PND 20.

With regard to Tacr3-immunoreactivity on PND 20, positive cells were mostly absent from the area lateral to the pyramidal cell layer of the CA1 region. There were no dose-related responses in any of DBDE, TBBPA, and HBCD studies (Fig. 4b).

Apoptotic cell indices in the SGZ

Few apoptotic bodies were found in the SGZ of the untreated controls in all studies at PND 20. In the DBDE study, no significant changes were observed at any dose at this time point. A slight but statistically significant increase was observed in the number of apoptotic bodies after exposure to 10,000 ppm TBBPA and 10,000 pm HBCD, as compared with their respective untreated controls (Fig. 5). However, on PND 77, we detected very few apoptotic bodies in any of the cases including the untreated controls without statistically significant differences in any of the DBDE, TBBPA, and HBCD studies (Fig. 5).

Discussion

In the present study, we found an increase in reelin-expressing interneurons in the dentate hilus of offspring of dams exposed to the middle and higher dose of DBDE and TBBPA or the middle dose of HBCD at the end of exposure on PND 20. We also observed an increase in apoptotic cells in the neuroblast-producing SGZ of the dentate gyrus after exposure to high doses of TBBPA and HBCD on this time point. Reelin functions on neuronal migration and

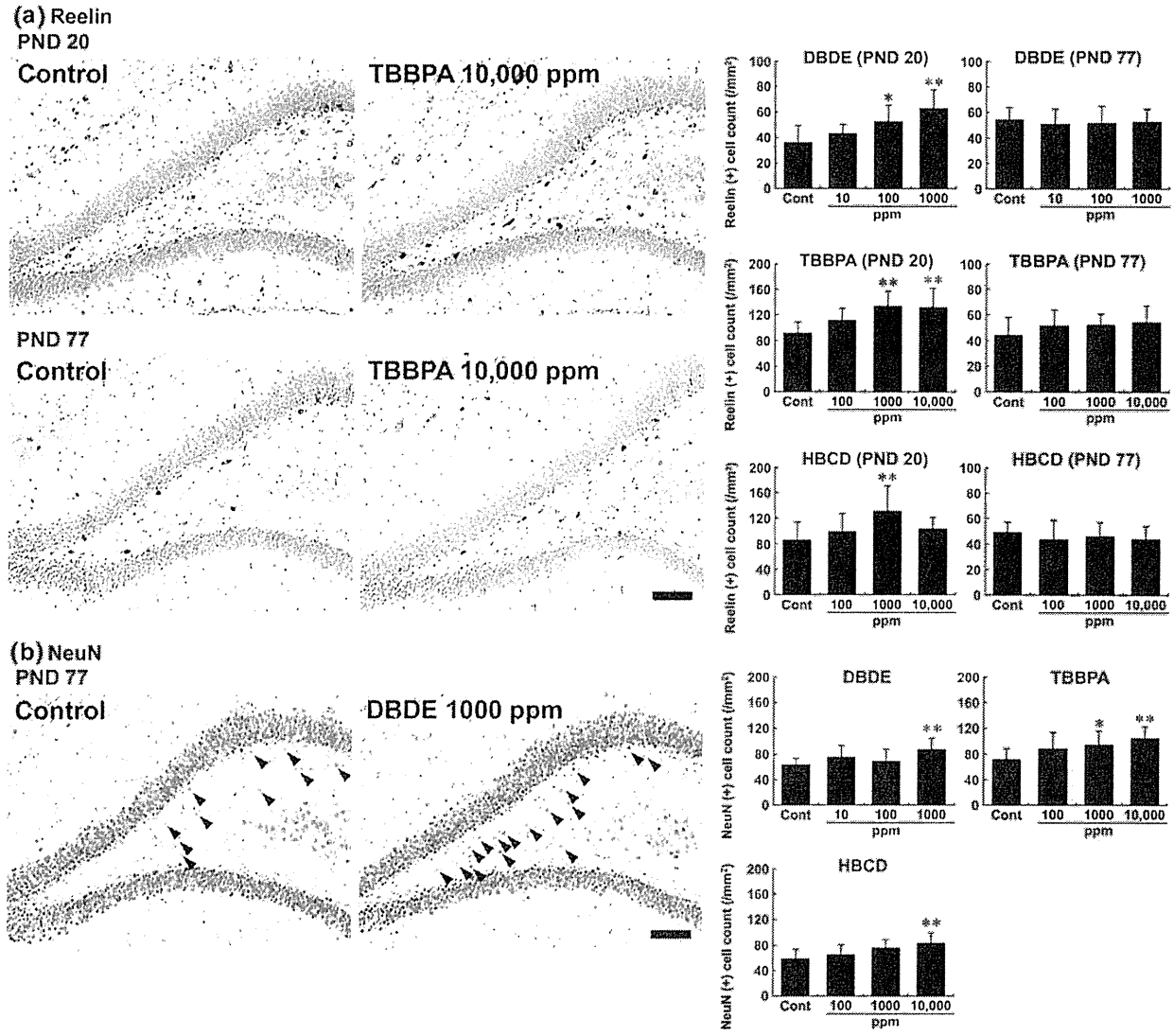

Fig. 2 Distribution of cells immunoreactive for reelin and NeuN in the hippocampal dentate gyrus in rat offspring after maternal exposure to DBDE, TBBPA, or HBCD. **a** Reelin-immunoreactive cells in the hilus of the dentate gyrus at PND 20 and PND 77. Reelin-positive cells with abundant cytoplasm show scattered distribution within the hilar region of the dentate gyrus. Note the higher number of reelin-positive cells in an animal exposed to 10,000 ppm TBBPA (*upper right*) compared with the control animal (*upper left*) on PND 20, while the number of reelin-positive cells in an animal in this group (*lower right*) at PND 77 was not different from the control animal (*lower left*). *Bar* = 100 μm. The graphs show the number of reelin-positive cells/unit area (mm^2) of the hilus of the bilateral hemispheres examined on both PND 20 and PND 77. Values were expressed as mean + SD. $N = 5$–14 in each group. $^*P < 0.05$, $^{**}P < 0.01$ versus controls (0 ppm) by Dunnett's test or Dunnett-type rank-sum test. **b** NeuN-immunoreactive cells as indicated with *arrowheads* at PND 77. NeuN-positive mature neurons are mainly distributed in the hilar area medial to the SGZ. Note the higher number of NeuN-positive cells in an animal exposed to 1,000 ppm DBDE (*right*) compared with the control animal (*left*). *Bar* = 100 μm. The graphs show the number of NeuN-positive cells/unit area (mm^2) of the hilus of the bilateral hemispheres on PND 77. Values were expressed as mean + SD. $N = 8$–10 in each group. $^*P < 0.05$, $^{**}P < 0.01$ versus controls (0 ppm) by Dunnett's test or Dunnett-type rank-sum test

positioning during brain development (D'Arcangelo et al. 1997; Alvarez-Dolado et al. 1999). Therefore, our observation that the increase in reelin-producing cells at the end of developmental exposure to BFRs might be a signature of a compensatory regulation mechanism for neuronal mismigration following impaired neurogenesis of the dentate granular cells. Similar results were found with the cases with developmental hypothyroidism in our previous study (Saegusa et al. 2010b).

Hoareau et al. (2006) reported that the transient prenatal disturbance of neurogenesis by treatment with methylazoxymethanol induces a long-term increase in the number of

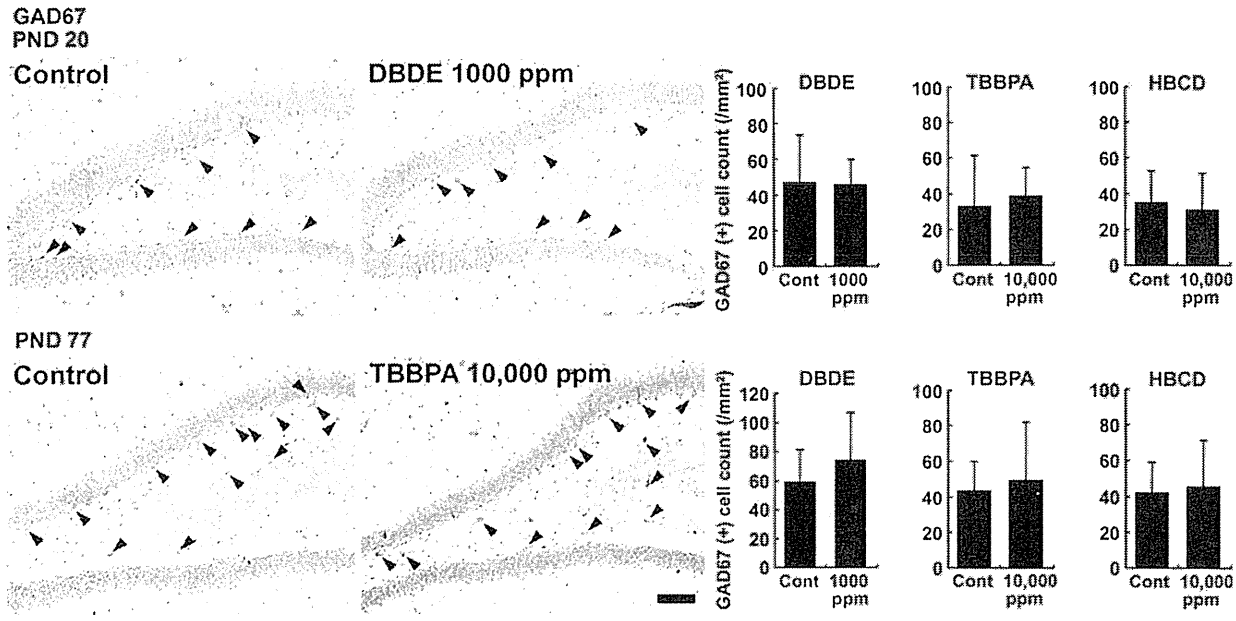

Fig. 3 Distribution of cells immunoreactive for GAD67 as indicated with *arrowheads* in the hilus of the dentate gyrus of rat offspring at PND 20 and PND 77 after maternal exposure to DBDE, TBBPA, or HBCD. *Bar* = 100 μm. The graphs show the number of GAD67-positive cells/unit area (mm^2) of the hilus of the bilateral hemispheres on both PND 20 and PND 77. Values were expressed as mean + SD. $N = 5$ in each group

reelin-expressing neurons in the hippocampus. In the present study, the number of reelin-producing cells in the hilus had returned to control levels on PND 77 in all experiments, which is different from the sustained increase after exposure to antithyroid agents we found previously (Saegusa et al. 2010b). Because reelin acts as a stop signal (Frotscher et al. 2003), the absence of excess population of reelin-expressing cells at later stages in the dentate hilus observed here could reflect a recovery to normal levels, to maintain the migration of the granular cells. Conversely, we found an increase in NeuN-positive mature neurons in the hilus after exposure to the middle and higher doses of TBBPA or the high dose of DBDE and HBCD on PND 77. We have also previously observed an increase in NeuN-positive mature neurons in addition to the sustained increase in reelin-expressing immature interneurons in the hilus by developmental hypothyroidism on PND 77 (Saegusa et al. 2010b), suggesting generation of an excess of mature neurons in the hilus as a sign of disruptive effect on neurogenesis and following neuronal migration during developmental exposure.

In the rodent dentate hilus, there are neurons other than GABAergic interneurons, in approximately equal numbers (Houser 2007). In the present study, we attempted to determine whether the increased number of NeuN-positive mature neurons were GABAergic interneurons. However, we did not observe fluctuations in the number of GAD67-positive cells at either PND 20 or PND 77 after BFR exposure. However, it has been reported that immunostaining with antibodies against GAD65 and GAD67 often produces inconsistencies between the antibodies, which makes it difficult to demonstrate an entire population of GABAergic interneurons (Houser 2007). This means that the cellular identity of NeuN-positive mature neurons in the present study remains unclear. Considering that reelin is an inducible molecule and its expression level can be modified during the disease process (Kundakovic et al. 2009; Stein et al. 2010), it may be reasonable to consider that the excess population of reelin-producing interneurons during the exposure to BFR halted their reelin production after the exposure ended, reflecting a recovery from the neuronal effects. While the biological significance should be assessed in further studies, the increase in mature neurons in the dentate gyrus at later stages may be the signature of the effects of chemical exposure during the developmental stages. As no changes were found in the distribution of CA1 pyramidal neurons and the number of reelin-expressing cells was reversible, the effects of BFRs on neuronal development is judged to be weak compared with those of antithyroid agents (Saegusa et al. 2010b).

Both thyrotoxic effects (Rice et al. 2007; Tseng et al. 2008) and developmental neurobehavioral effects (Rice et al. 2007) were reported in mice after exposure to DBDE, but no studies have been carried out in rats. In the present study, the offspring exposed to 1,000 ppm DBDE showed a slight decrease in serum triiodothyronine (T_3)

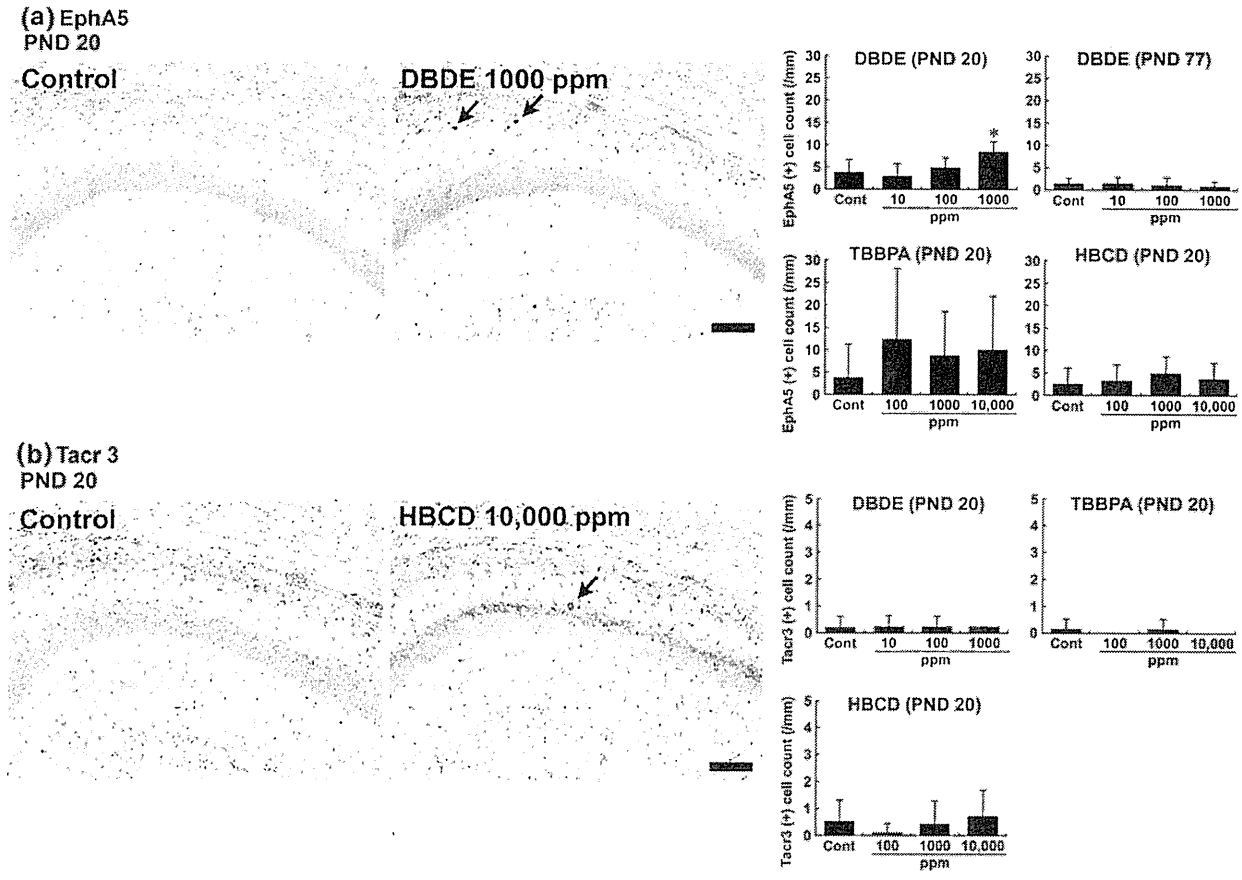

Fig. 4 Distribution of cells immunoreactive for EphA5 and Tacr3 in the hippocampal formation in rat offspring after maternal exposure to DBDE, TBBPA, or HBCD. **a** EphA5-immunoreactive cells located in the stratum oriens of the CA1 region on PND 20. *Bar* = 100 μm. Note a few EphA5-positive cells (*arrows*) in an animal exposed to 1,000 ppm DBDE (*right*) compared with no positive cells in a control animal (*left*). The graph shows the number of EphA5-positive cells/unit length (mm) of the CA1 region of the bilateral hemispheres on PND 20 or PND 77. Values were expressed as mean + SD. $N = 5$–10 in each group. $^*P < 0.05$ versus controls (0 ppm) by Dunnett's test or Dunnett-type rank-sum test. **b** Tacr3-immunoreactive cells located within the pyramidal cell layer and stratum oriens of the CA1 region on PND 20. *Bar* = 100 μm. Note one Tacr3-positive cell (*arrow*) in an animal exposed to 10,000 ppm HBCD (*right*). The graph shows the number of Tacr3-positive cells/unit length (mm) of the CA1 region of bilateral hemispheres on PND 20. Values were expressed as mean + SD. $N = 5$–10 in each group

concentrations accompanied with increase in the incidence of thyroid follicular cell hypertrophy on PND 20 (Fujimoto et al. 2011; Online Resource 1, Table s1). While we also observed non-significant increase in incidence of thyroid follicular cell hypertrophy in all exposure groups (Fujimoto et al. 2011), these results may suggest that DBDE at least at 1,000 ppm caused mild developmental hypothyroidism that was sustained until adult stage. Zhang et al. (2011) recently reported tissue distribution including the brain of DBDE and its debrominated metabolites in sucking rat pups after prenatal and/or postnatal exposure, suggesting a possibility of direct effect of DBDE on neuronal development. A relationship between the accumulation of DBDE in the brain and changes in spontaneous behavior was reported in mice after a single neonatal administration of DBDE (20.1 mg/kg body weight by oral gavage) on day 3 after birth, suggesting the possibility of a direct chemical effect on the neuronal development in the brain (Viberg et al. 2003); however, questions have been raised by others on the analytical methodology applied and data calculation (Vijverberg and van den Berg 2004; Goodman 2009). A similar neurobehavioral effects were observed in rats after a single administration of the same dose, but thyrotoxic effects were not examined (Viberg et al. 2007). In the present study, we observed an increase in reelin-expressing interneurons after exposure to DBDE of 100 ppm (7.0–22.8 mg/kg body weight/day) and higher on PND 20, suggesting primarily a direct effect of DBDE on neuronal development accompanied with hypothyroidism-related effect at 1,000 ppm. In another recent study, Ibhazehiebo et al. (2011a) reported disruption of TH-mediated transcription by DBDE in a reporter gene assay. Such effect